Limited-angle tomography

Samuli Siltanen

PhD Winter School 2023

Advanced methods for mathematical image analysis

Bologna, Italy

January 25, 2023

Instagram:
@samuntiede
@monday_spider

YouTube:
@professor_sam
@Samuntiedekanava

Outline

Where do we encounter limited-angle tomography?

Industrial case study: low-dose 3D dental X-ray imaging

Matrix-based limited angle tomography and SVD

Ill-posedness of limited-angle Radon transform

Recent progress in limited-angle tomography
- Learning the unknown WF set with shearlets
- Learning the unknown WF set with complex wavelets
- Estimating the unknown WF set with computational topology

Helsinki tomography challenge 2022

In 3D mammography, the imaging geometry restricts the angular range of the data

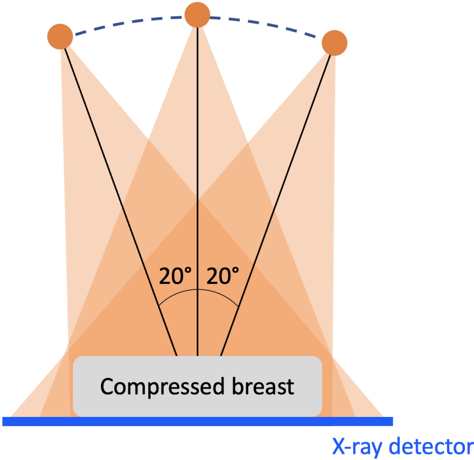

Paralle slices in the reconstruction can be improved with Bayesian inversion

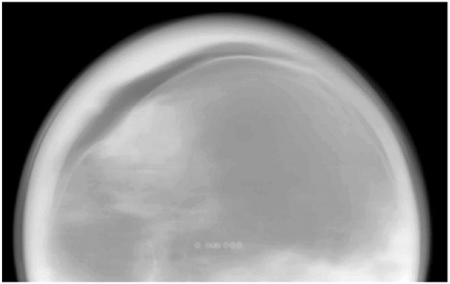

Tomosynthesis

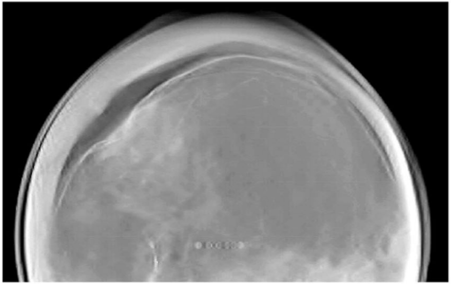

MAP estimate with Besov prior, $p = 1.5 = q$ and $s = 0.5$

[Rantala et al. (2006), US patent 7215730]

This part is a joint work with

Alexander Meaney, University of Helsinki, Finland

Esa Niemi, Eniram Ltd., Finland

Aaro Salosensaari, University of Helsinki, Finland

Industrial partners:

Kemppi Ltd. (welding tool manufacturer)

Ajat Ltd. (X-ray detector manufacturer)

Two steel pipes partly welded together


0.5


0.5

This is the limited-angle measurement geometry for a narrow CaTd direct conversion detector

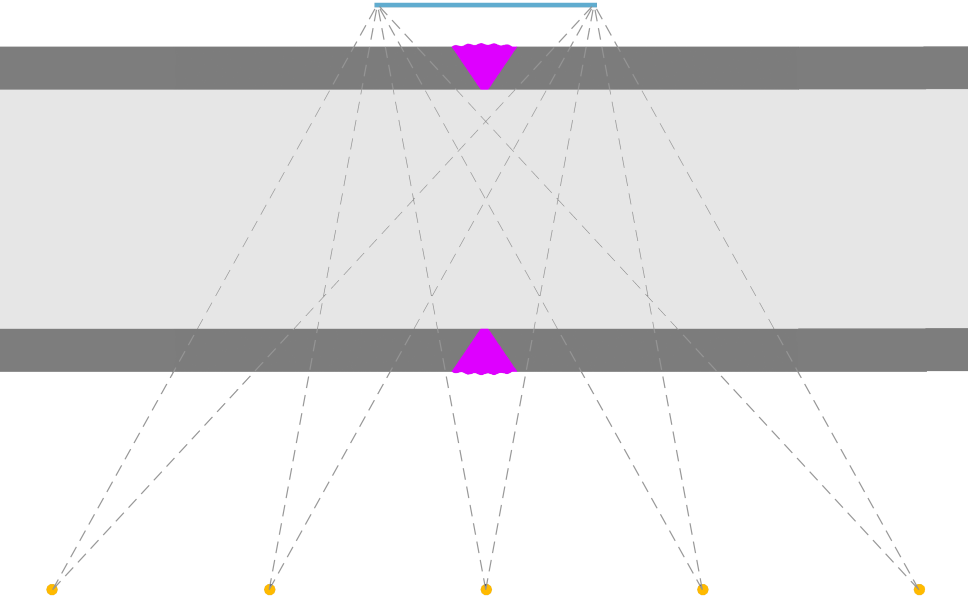

Traditional reconstruction by tomosynthesis

Simulated phantom:

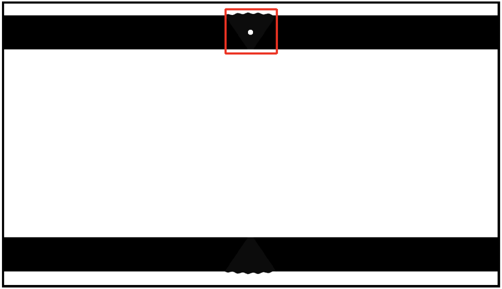

Tomosynthesis:

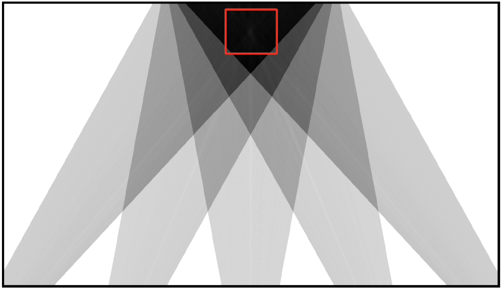

TVR-DART with domain restriction

Simulated phantom:

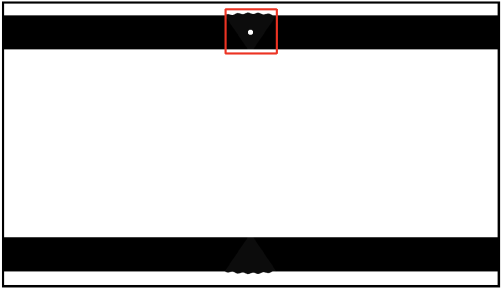

TVR-DART:

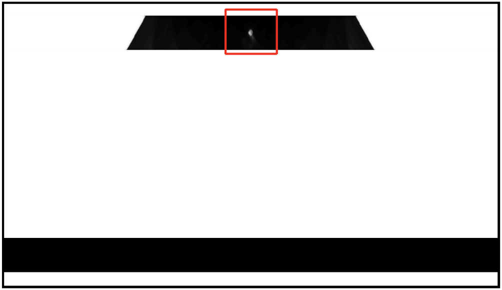

Reconstructions from measured data

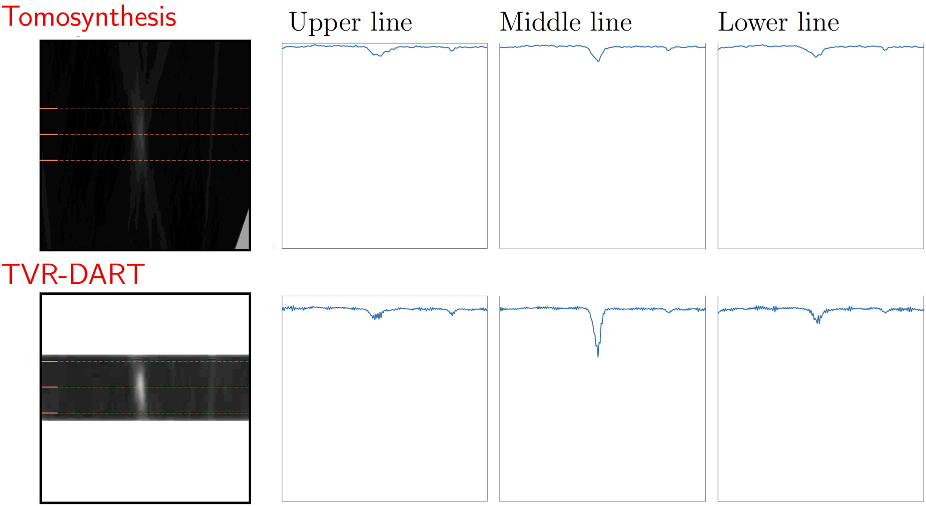

[Niemi, Salosensaari, Meaney & S, submitted manuscript]

Tomography appears in adaptive optics

- Modern telescope imaging suffers from turbulence in the atmosphere
  $\Rightarrow$ blurring of images
- Adaptive optics corrects the perturbed incoming light in real-time
- Major challenge in wide-field AO: atmospheric tomography

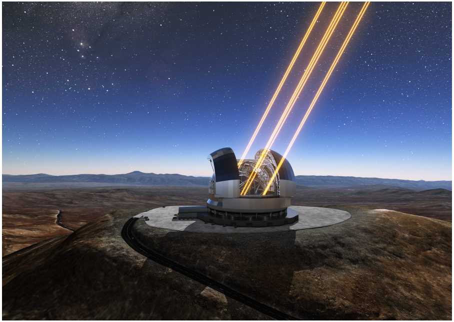

European Extremely Large Telescope (2024)

Helin, Kindermann, Lehtonen & Ramlau 2018
Yudytskiy, Helin & Ramlau 2014

Photograph of planet Neptune with and without adaptive optics (image: ESO/P. Weilbacher)

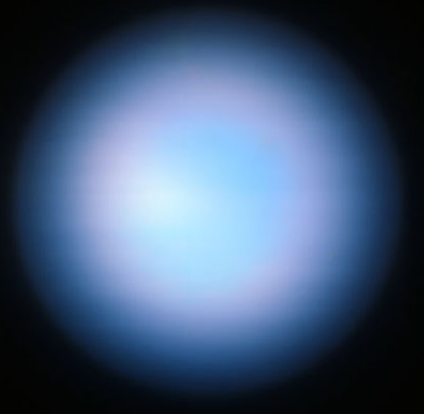

No adaptive optics

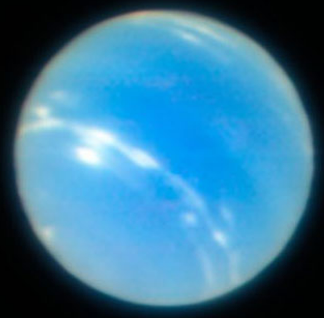

Adaptive optics

Outline

Where do we encounter limited-angle tomography?

Industrial case study: low-dose 3D dental X-ray imaging

Matrix-based limited angle tomography and SVD

Ill-posedness of limited-angle Radon transform

Recent progress in limited-angle tomography
- Learning the unknown WF set with shearlets
- Learning the unknown WF set with complex wavelets
- Estimating the unknown WF set with computational topology

Helsinki tomography challenge 2022

Application: dental implant planning, where a missing tooth is replaced with an implant

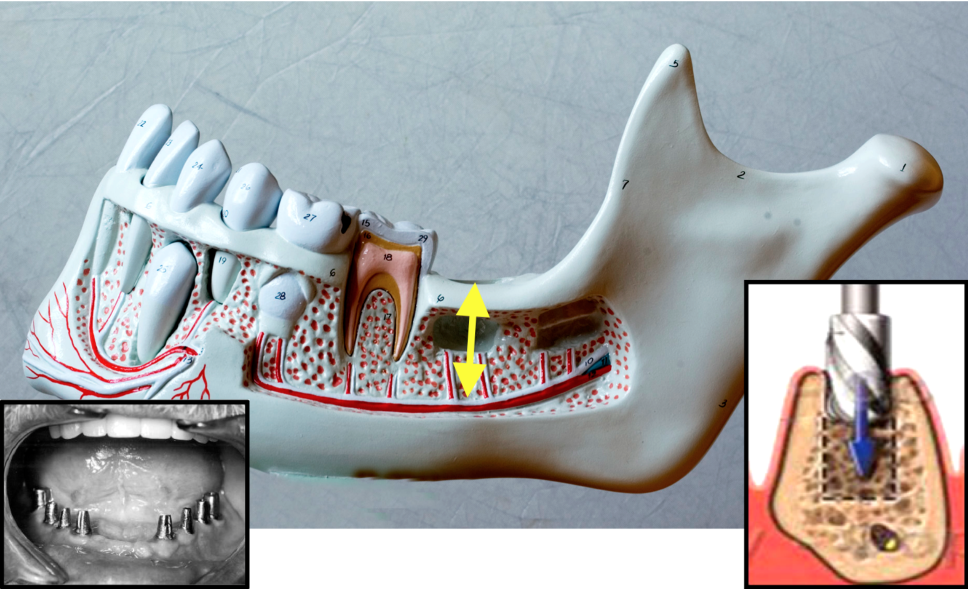

This is the classical imaging procedure of the panoramic X-ray device

The resulting image shows a sharp layer positioned inside the dental arc

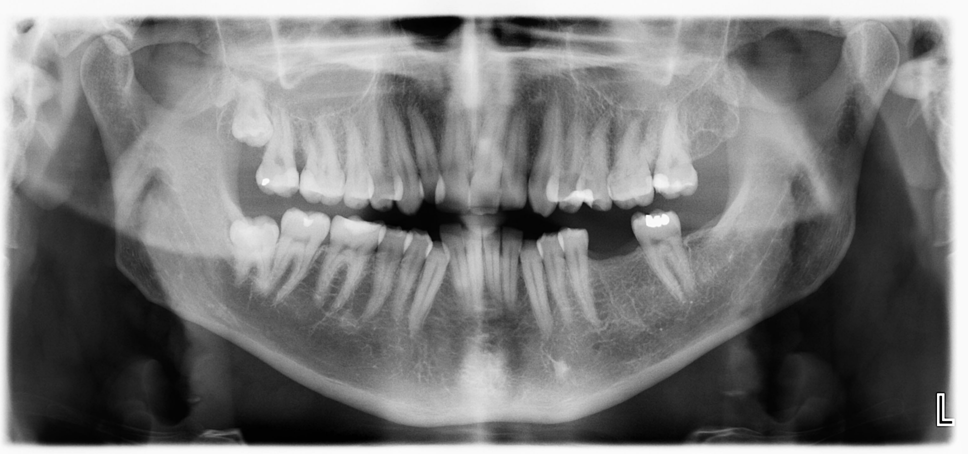

Nowadays, a digital panoramic imaging device is standard equipment at dental clinics

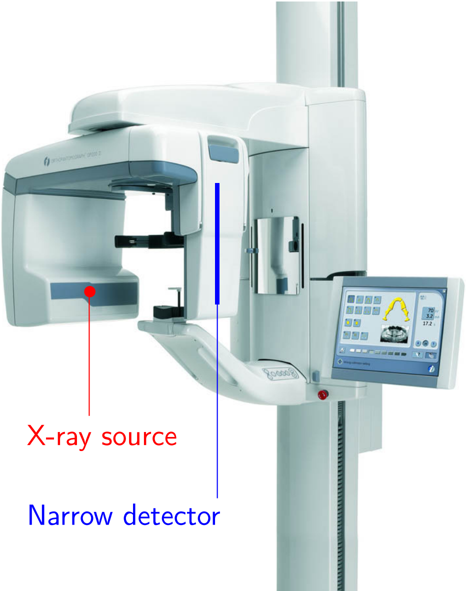

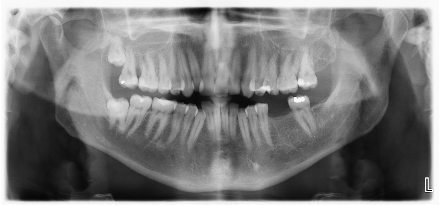

A panoramic dental image offers a general overview showing all teeth and other structures simultaneously.

Panoramic images are not suitable for dental implant planning because of unavoidable geometric distortion.

We reprogram the panoramic X-ray device so that it collects projection data by scanning

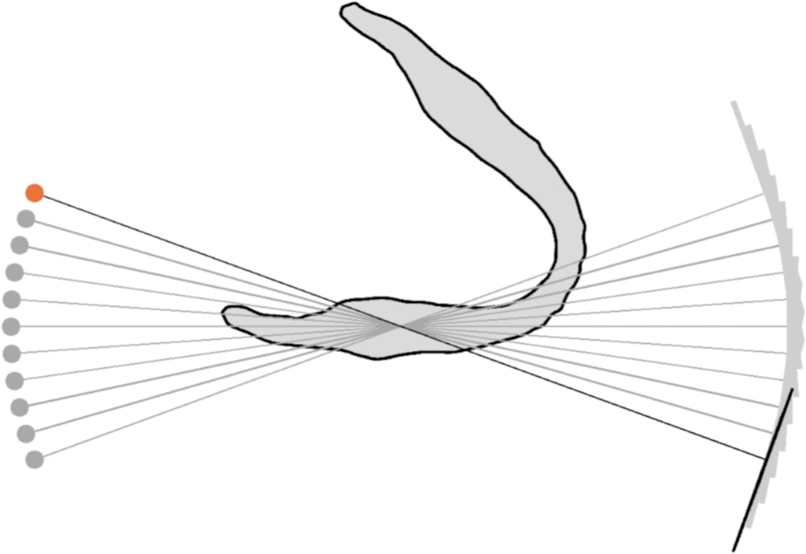

We reprogram the panoramic X-ray device so that it collects projection data by scanning

Number of projection images: **11**

Angle of view: **40 degrees**

Image size: **1000×1000 pixels**

The unknown vector f has **7 000 000** elements.

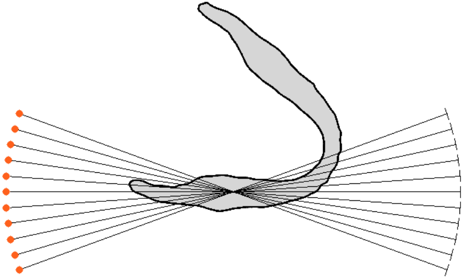

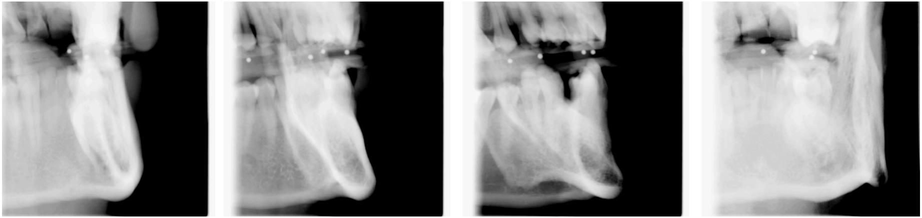

Standard Cone Beam CT reconstruction delivers 100 times more radiation than VT imaging

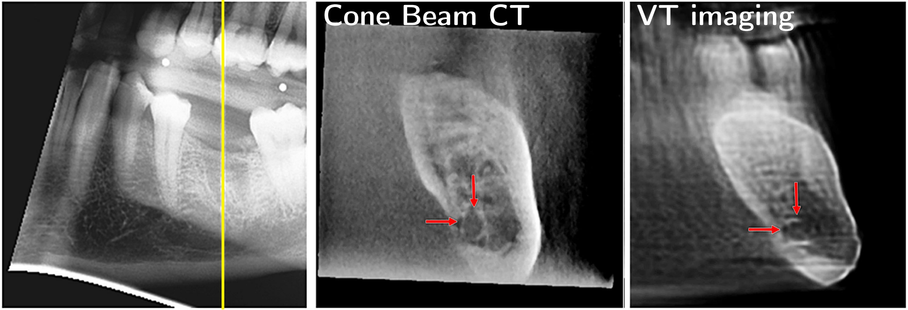

Kolehmainen, Vanne, S, Järvenpää, Kaipio, Lassas & Kalke **2006**

Kolehmainen, Lassas & S **2008**

Cederlund, Kalke & Welander **2009**

Hyvönen, Kalke, Lassas, Setälä & S **2010**

U.S. patent 7269241, thousands of VT units in use

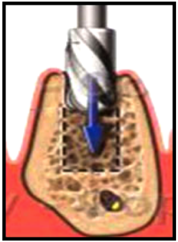

The VT device was developed in 2001–2012 by

Nuutti Hyvönen
Seppo Järvenpää
Jari Kaipio
Martti Kalke
Petri Koistinen
Ville Kolehmainen
Matti Lassas
Jan Moberg
Kati Niinimäki
Juha Pirttilä
Maaria Rantala
Eero Saksman
Henri Setälä
Erkki Somersalo
Antti Vanne
Simopekka Vänskä
Richard L. Webber

Outline

Where do we encounter limited-angle tomography?

Industrial case study: low-dose 3D dental X-ray imaging

Matrix-based limited angle tomography and SVD

Ill-posedness of limited-angle Radon transform

Recent progress in limited-angle tomography
- Learning the unknown WF set with shearlets
- Learning the unknown WF set with complex wavelets
- Estimating the unknown WF set with computational topology

Helsinki tomography challenge 2022

Discretize the unknown by dividing it into pixels

Target (unknown)

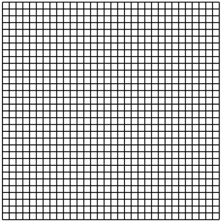

32×32 pixel grid

Construction of limited-angle sinogram

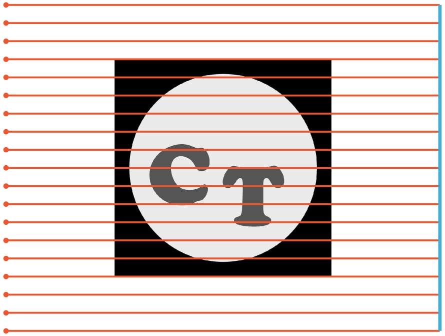

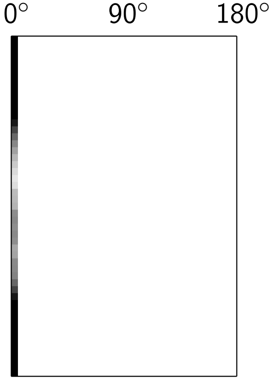

Construction of limited-angle sinogram

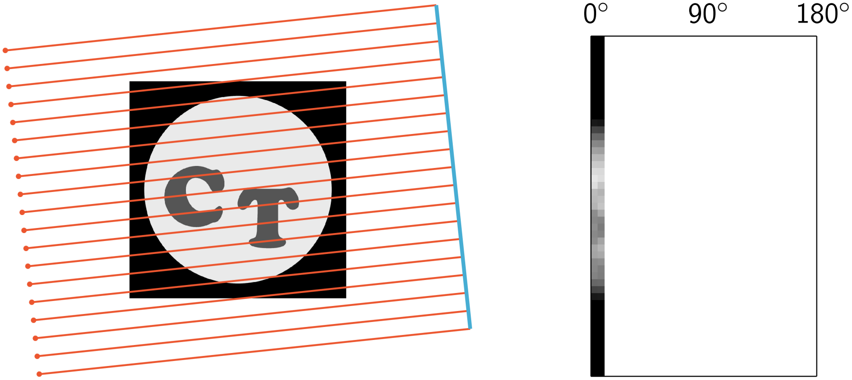

Construction of limited-angle sinogram

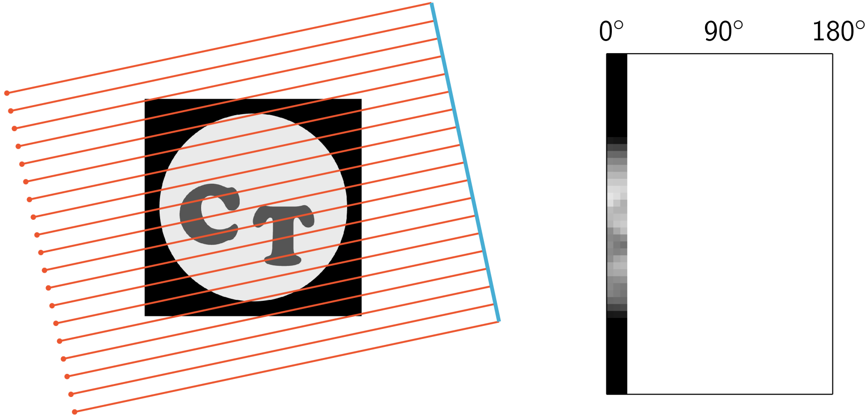

Construction of limited-angle sinogram

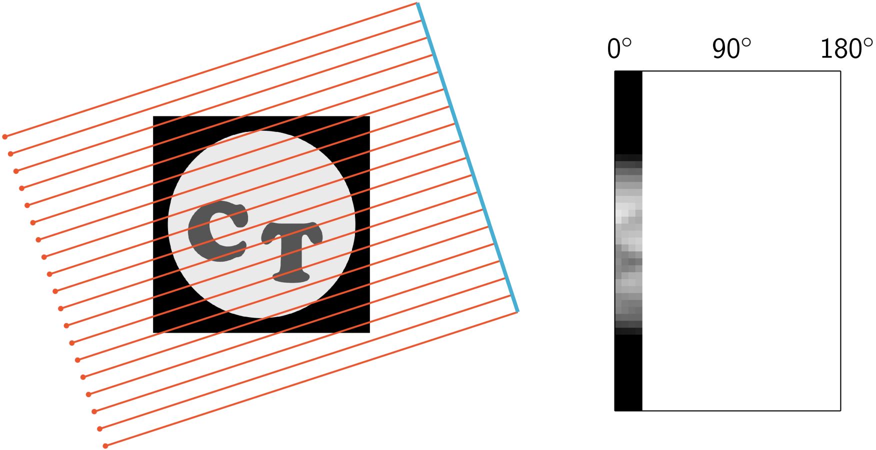

Construction of limited-angle sinogram

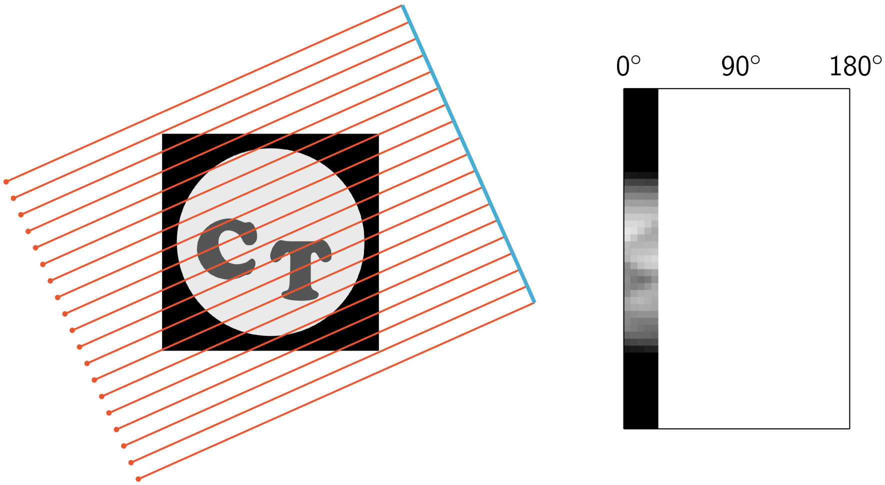

Construction of limited-angle sinogram

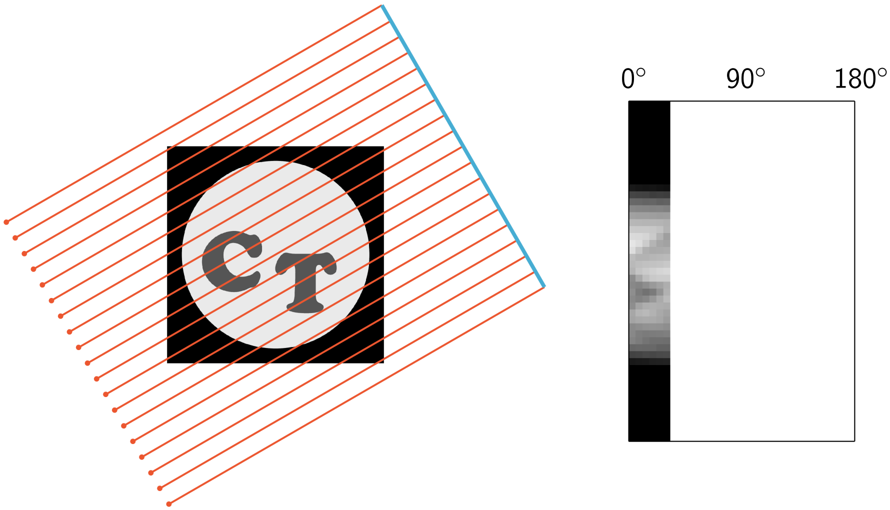

Construction of limited-angle sinogram

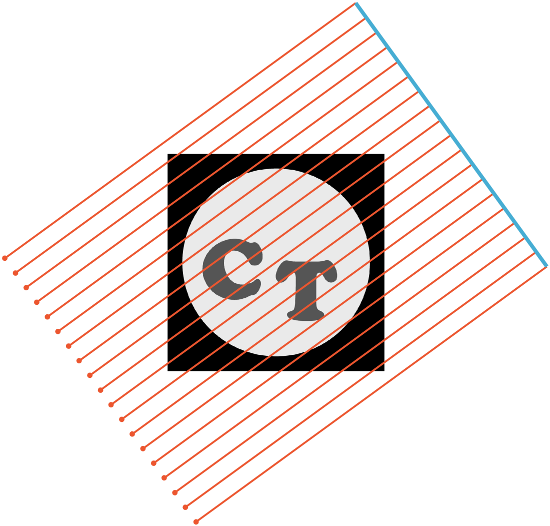

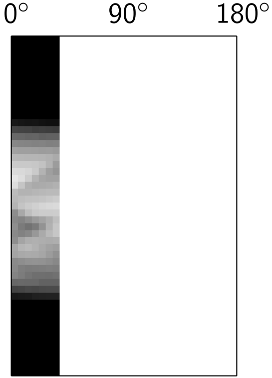

Construction of limited-angle sinogram

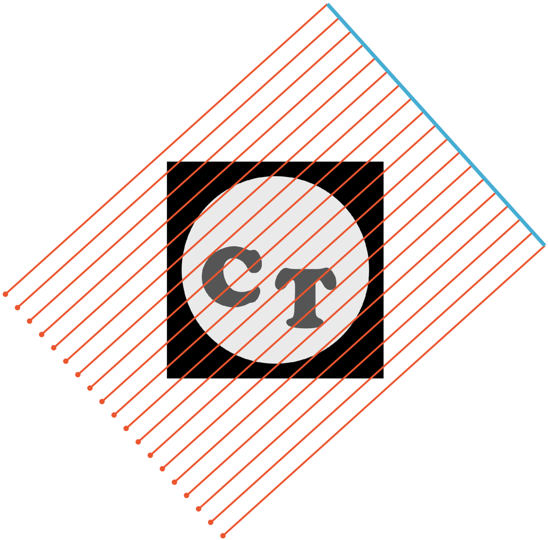

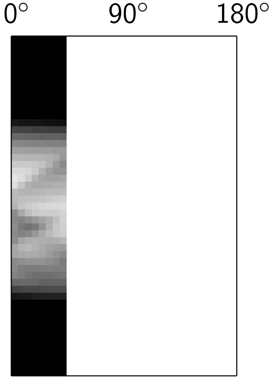

Construction of limited-angle sinogram

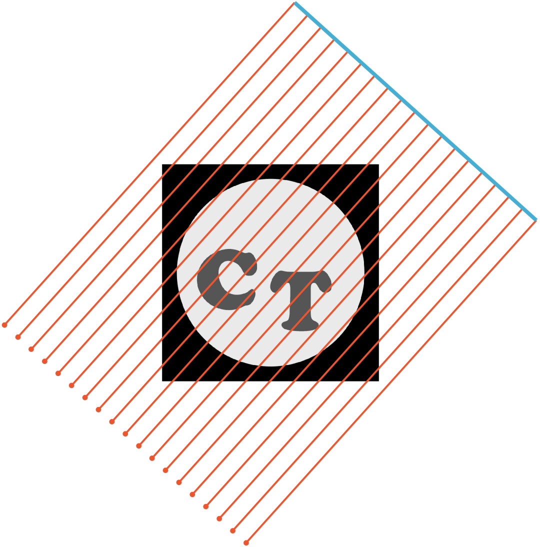

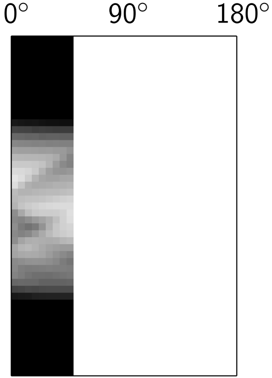

Construction of limited-angle sinogram

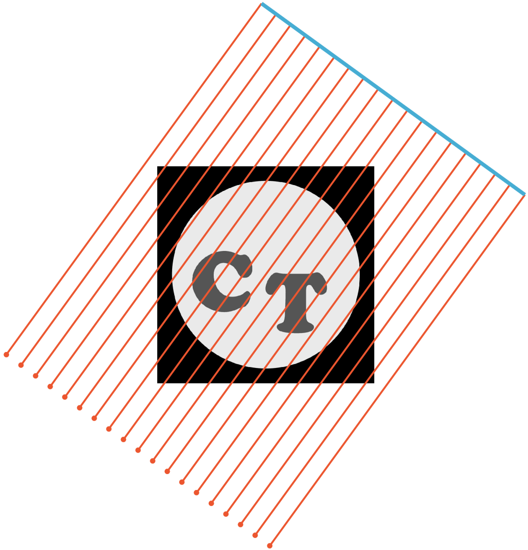

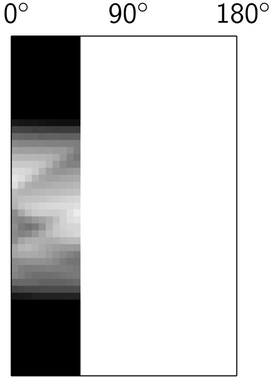

Construction of limited-angle sinogram

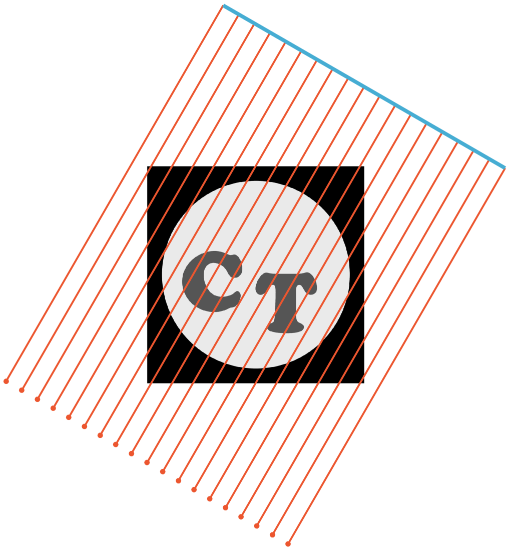

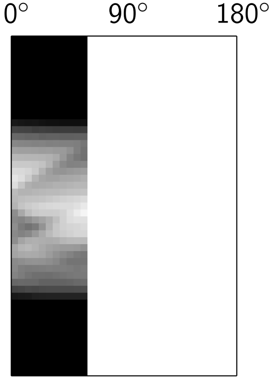

Construction of limited-angle sinogram

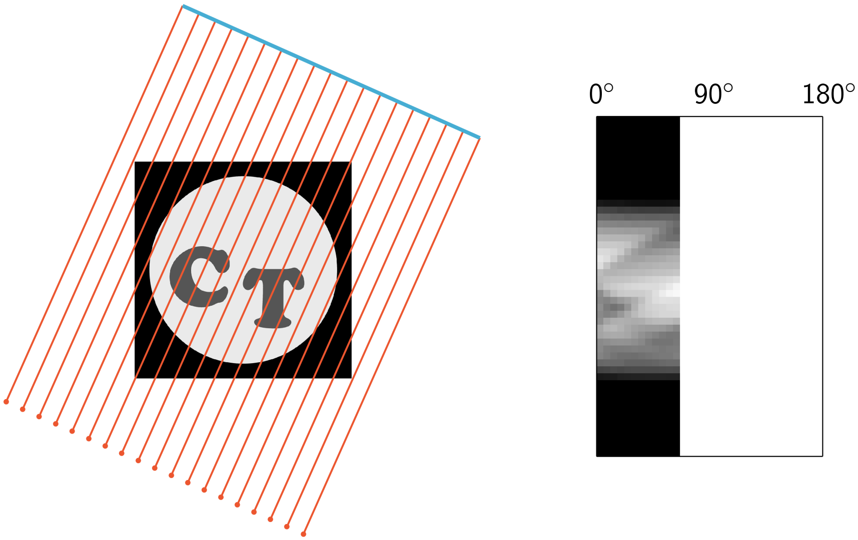

Construction of limited-angle sinogram

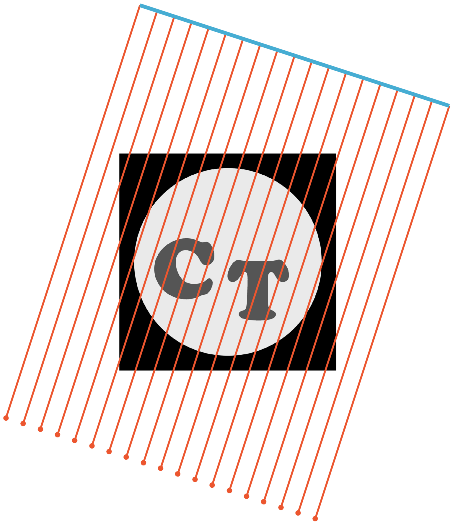

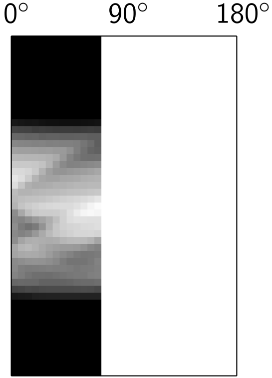

Construction of limited-angle sinogram

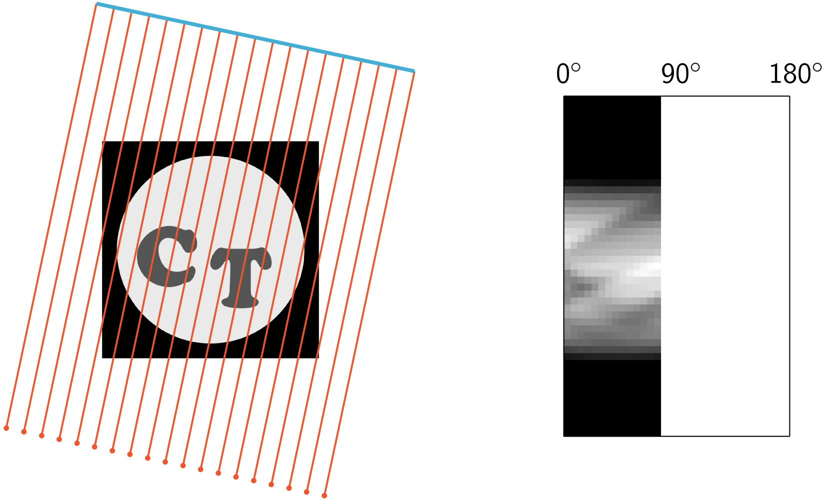

Construction of limited-angle sinogram

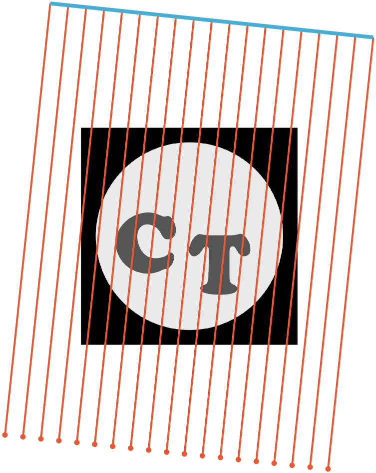

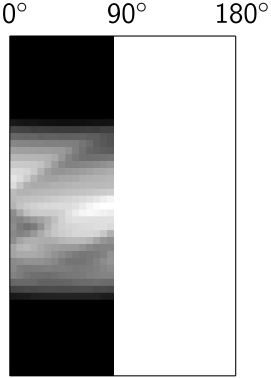

SVD reveals the ill-posedness of the limited-angle problem, see Davison 1983 and Louis 1986

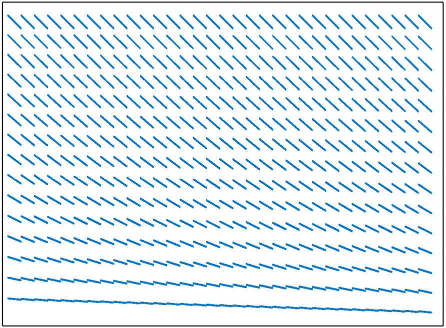

735×1024 system matrix A, only nonzero elements shown

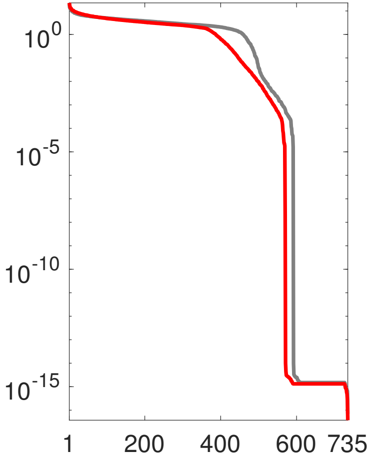

Singular values of A (diagonal of D)

Filtered Back-Projection (FBP) reconstruction from limited-angle data

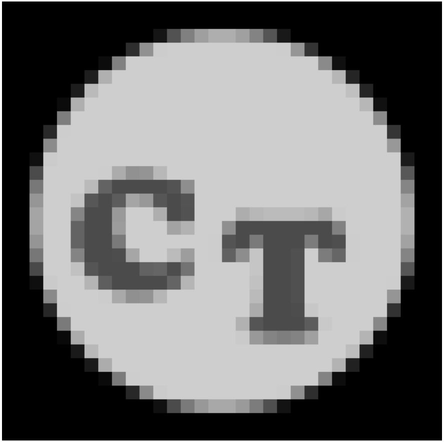

Original phantom sampled at 32×32 resolution

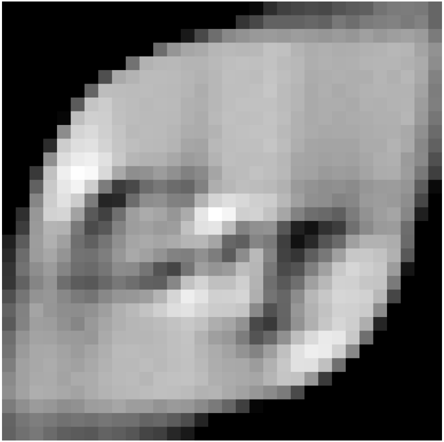

Filtered back-projection

Non-negative Tikhonov regularization

$$\underset{f \in \mathbb{R}^n_+}{\arg\min} \left\{ \|Af - m\|_2^2 + \alpha \|f\|_2^2 \right\}$$

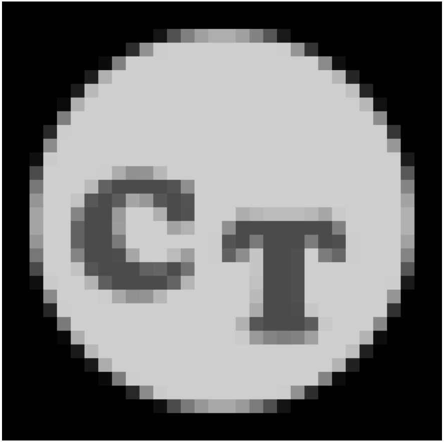

Original phantom sampled at 32×32 resolution

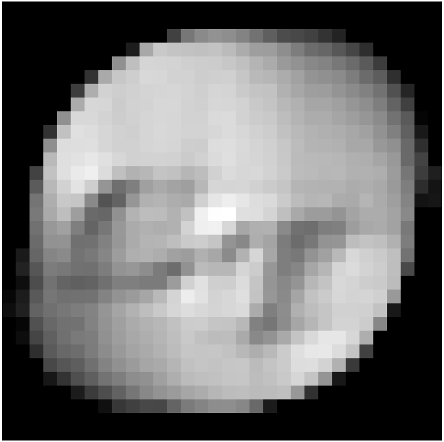

Tikhonov regularized reconstruction

Non-negative limited-angle TV regularization

$$\arg\min_{f \in \mathbb{R}^n_+} \left\{ \|Af - m\|_2^2 + \alpha \|\nabla f\|_1 \right\}$$

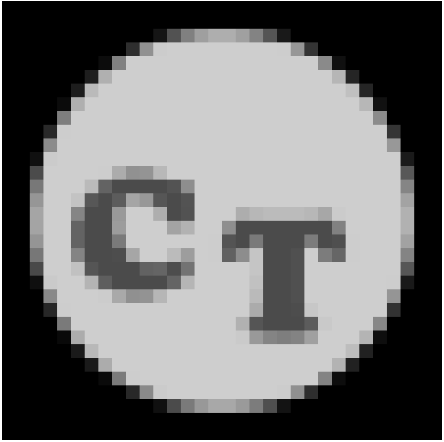

Original phantom sampled at 32×32 resolution

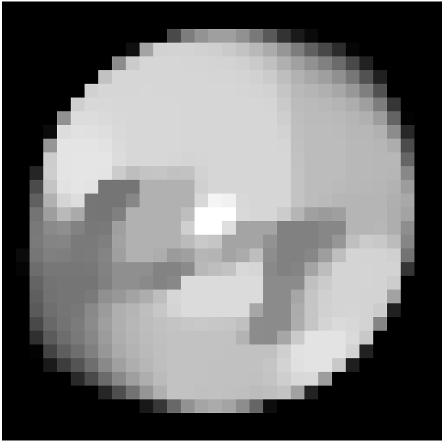

TV reconstruction

Outline

Where do we encounter limited-angle tomography?

Industrial case study: low-dose 3D dental X-ray imaging

Matrix-based limited angle tomography and SVD

Ill-posedness of limited-angle Radon transform

Recent progress in limited-angle tomography
- Learning the unknown WF set with shearlets
- Learning the unknown WF set with complex wavelets
- Estimating the unknown WF set with computational topology

Helsinki tomography challenge 2022

A of Continuous Theory

Definition of the Radon transform

Let $f(x) = f(x_1, x_2)$ be the X-ray attenuation coefficient. The classical model for tomographic data is the Radon transform

$$Rf(\theta, s) = \int_{x\cdot\vec{\theta}=s} f(x)dx = \int_{\tau\in\mathbb{R}} f(s\vec{\theta}+\tau\vec{\theta}^{\perp})d\tau, \qquad \vec{\theta} \in S^1, s \in \mathbb{R},$$

where S^1 is the unit circle, $\vec{\theta}^{\perp}$ is a unit vector perpendicular to the unit vector $\vec{\theta} = (\cos\theta, \sin\theta)$, and $x \cdot \vec{\theta}$ denotes vector inner product.

Note that f is defined on $\mathbb{R}^2$ and Rf is defined on $S^1 \times \mathbb{R}^1$.

The Fourier slice theorem

Let $f : \mathbb{R}^2 \to \mathbb{R}$ be smooth and compactly supported. Denote $R_\theta f(s) := Rf(\theta, s)$ for $\vec{\theta} \in S^1$ and $s \in \mathbb{R}$. Then

$$\widehat{R_\theta f}(\xi) = \widehat{f}(\xi\vec{\theta}).$$

Proof. The change of coordinates $x = s\vec{\theta} + \tau\vec{\theta}^\perp$ gives $s = \vec{\theta} \cdot x$ and $dx = d\tau\, ds$. Calculate

$$\begin{aligned}
\widehat{R_\theta f}(\xi) &= \int_{-\infty}^{\infty} e^{-i\xi s} R_\theta f(s)\, ds \\
&= \int_{-\infty}^{\infty} e^{-i\xi s} \int_{-\infty}^{\infty} f(s\vec{\theta} + \tau\vec{\theta}^\perp) d\tau\, ds \\
&= \int_{\mathbb{R}^2} e^{-i\xi\vec{\theta}\cdot x} f(x) dx \\
&= \widehat{f}(\xi\theta). \qquad \square
\end{aligned}$$

Practically Dubious Theorem: Unique determination from limited-angle data

Let $f : \mathbb{R}^2 \to \mathbb{R}$ be smooth and compactly supported. Let $\varepsilon > 0$. Then f is uniquely determined from the limited-angle sinogram

$$Rf(\theta, s) \qquad \text{with } -\varepsilon < \theta < \varepsilon \text{ and } s \in \mathbb{R}.$$

Proof. Let f and g be compactly supported smooth functions defined on $\mathbb{R}^2$ satisfying $Rf(\theta, s) = Rg(\theta, s)$ for $-\varepsilon < \theta < \varepsilon$. By the Fourier slice theorem we know that

$$\widehat{f}(\xi\vec{\theta}) \equiv \widehat{g}(\xi\vec{\theta})$$

in the open set $C_\varepsilon := \{(\xi, \theta) \in \mathbb{R}^2 \,|\, \xi > 0,\ -\varepsilon < \theta < \varepsilon\}$. The Fourier transform of a compactly supported smooth function is analytic. So $\widehat{f} = \widehat{g}$ on the open set C_ε, and due to analyticity $\widehat{f} = \widehat{g}$ on the whole frequency domain $\mathbb{R}^2$. Therefore $f \equiv g$. $\square$

Limited angle measurement information looks like a bowtie in the frequency domain

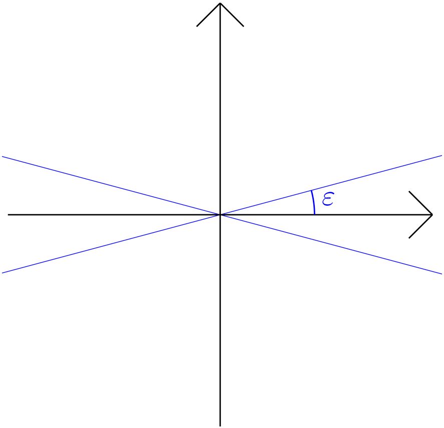

Range of measured angles is $(-\varepsilon, \varepsilon)$

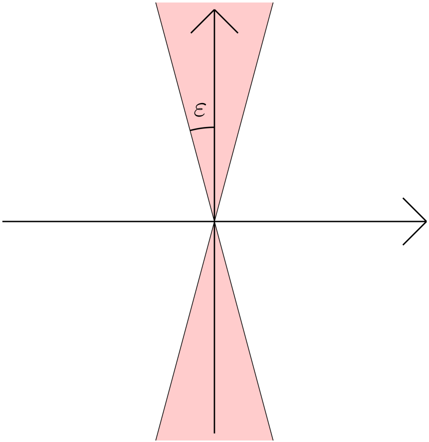

Frequency domain

What do we know about the singular values of the Radon transform?

Roughly speaking,

- the full-angle Radon transform allows a singular system where the singular values decay as $d_n \sim 1/n$ when $n \to \infty$;
- the singular values of limited-angle Radon transform decay exponentially even if the interval of missing angles is just $(-\varepsilon, \varepsilon)$ with any $\varepsilon > 0$.

The details are available in Natterer 1986, Sections IV.3 and VI.2.

For more information, see Davison 1983 and Louis 1986.

Limited data gives only part of the wavefront set

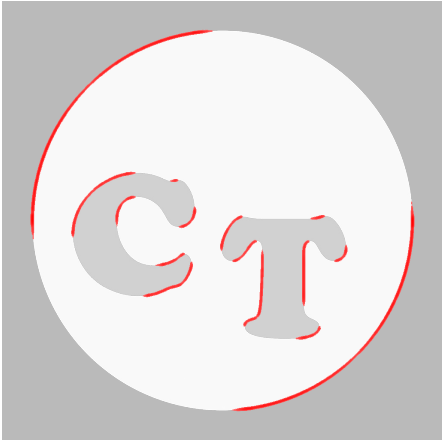

Stable part of wavefront set

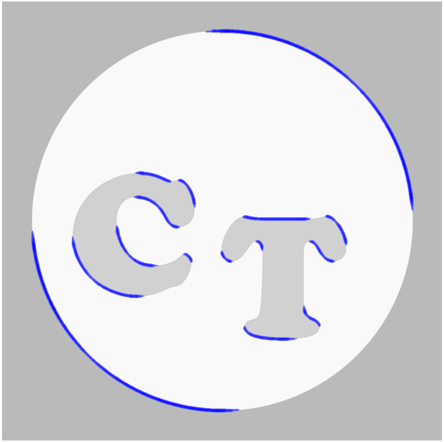

Unstable part of wavefront set

See [Greenleaf & Uhlmann 1989], [Quinto 1993], and [Frikel & Quinto 2013]

Filtered Back-Projection (FBP) reconstruction from limited-angle data

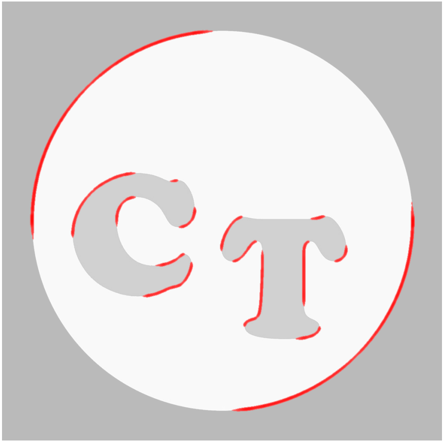

Stable part of wavefront set

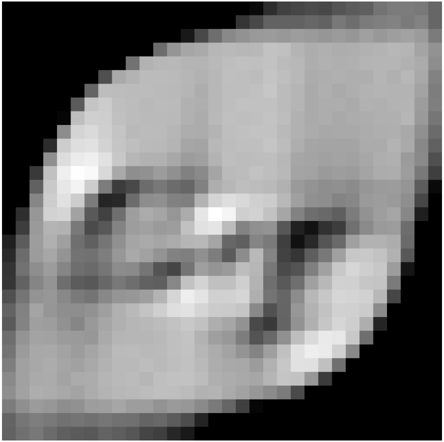

Filtered back-projection

Non-negative Tikhonov regularization

$$\underset{f\in\mathbb{R}^n_+}{\arg\min}\left\{\|Af-m\|_2^2+\alpha\|f\|_2^2\right\}$$

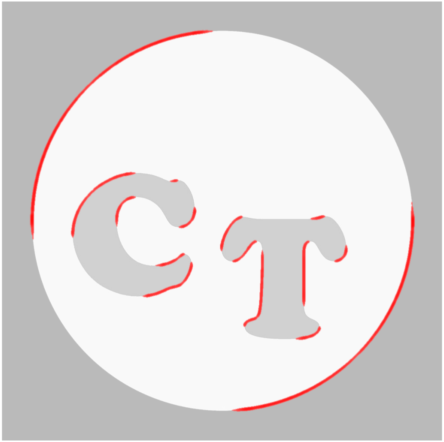

Stable part of wavefront set

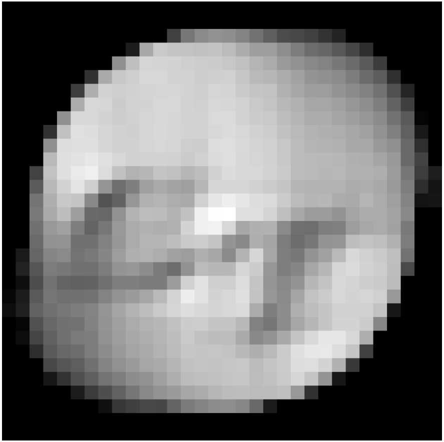

Tikhonov regularized reconstruction

Constrained total variation (TV) regularization

$$\operatorname*{arg\,min}_{f \in \mathbb{R}^n_+} \left\{ \|Af - m\|_2^2 + \alpha \|\nabla f\|_1 \right\}$$

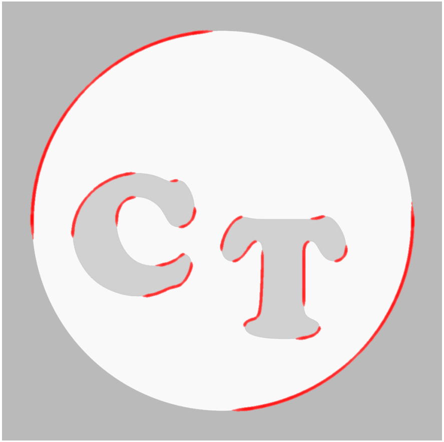

Stable part of wavefront set

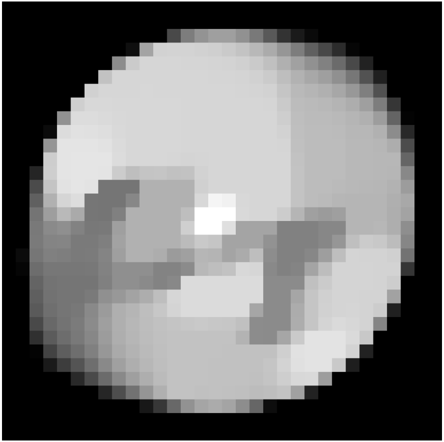

TV regularized reconstruction

Interesting papers that generalize the theme of detecting singularities

Borg, Frikel, Jørgensen and Quinto:
Analyzing Reconstruction Artifacts from Arbitrary Incomplete X-ray CT Data. Link.

Borg, Frikel, Jørgensen and Sporring:
Reduction of variable-truncation artifacts from beam occlusion during in situ *x-ray tomography*. Link.

Outline

Where do we encounter limited-angle tomography?

Industrial case study: low-dose 3D dental X-ray imaging

Matrix-based limited angle tomography and SVD

Ill-posedness of limited-angle Radon transform

Recent progress in limited-angle tomography

- Learning the unknown WF set with shearlets
- Learning the unknown WF set with complex wavelets
- Estimating the unknown WF set with computational topology

Helsinki tomography challenge 2022

Outline

Where do we encounter limited-angle tomography?

Industrial case study: low-dose 3D dental X-ray imaging

Matrix-based limited angle tomography and SVD

Ill-posedness of limited-angle Radon transform

Recent progress in limited-angle tomography
- Learning the unknown WF set with shearlets
- Learning the unknown WF set with complex wavelets
- Estimating the unknown WF set with computational topology

Helsinki tomography challenge 2022

Filtered back-projection fails to recover the invisible parts of boundaries

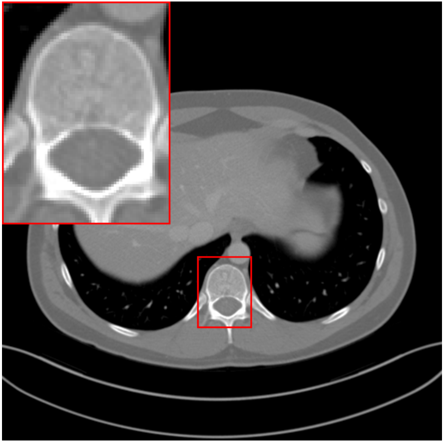

Ground truth

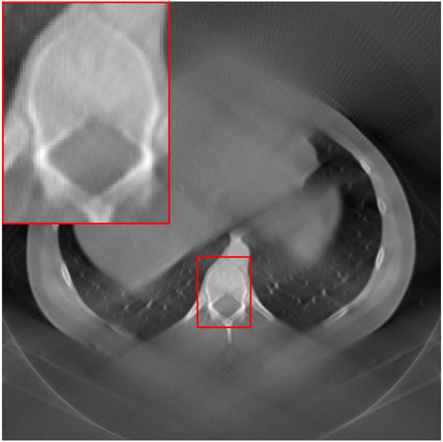

Filtered back-projection

When we learn the invisible parts of boundaries we can recover them

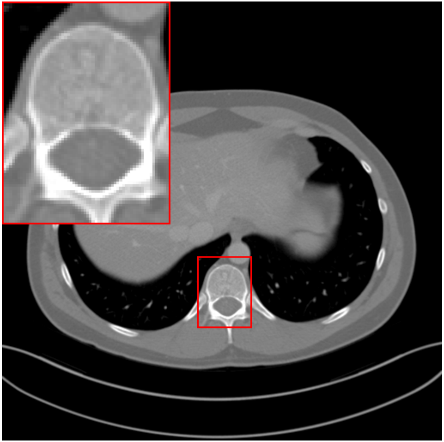

Ground truth

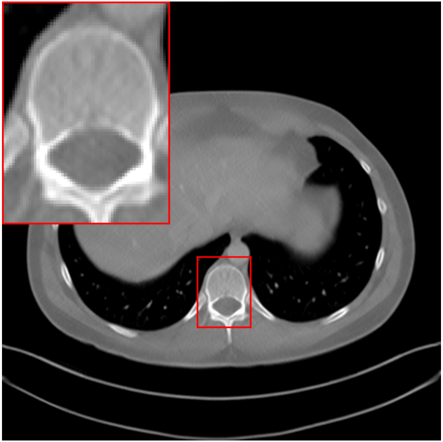

Invisible parts learned

[Bubba, Kutyniok, Lassas, Maerz, Samek, Siltanen and Srinivasan, *Inverse Problems* 2019]

Outline

Where do we encounter limited-angle tomography?

Industrial case study: low-dose 3D dental X-ray imaging

Matrix-based limited angle tomography and SVD

Ill-posedness of limited-angle Radon transform

Recent progress in limited-angle tomography

- Learning the unknown WF set with shearlets
- Learning the unknown WF set with complex wavelets
- Estimating the unknown WF set with computational topology

Helsinki tomography challenge 2022

Process pipeline invented by Siiri Rautio

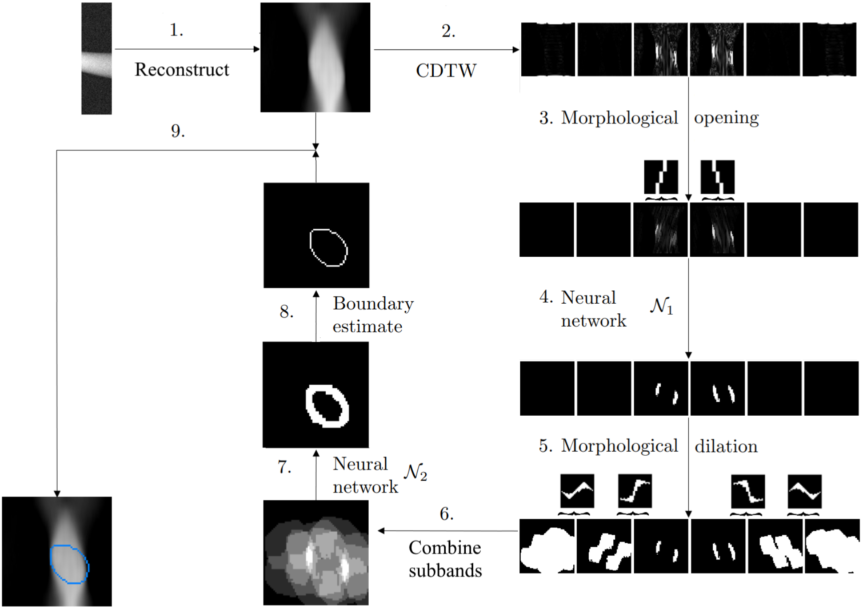

Machine learning grasps "candy-wrap" geometry of complex dual-tree wavelet coefficients

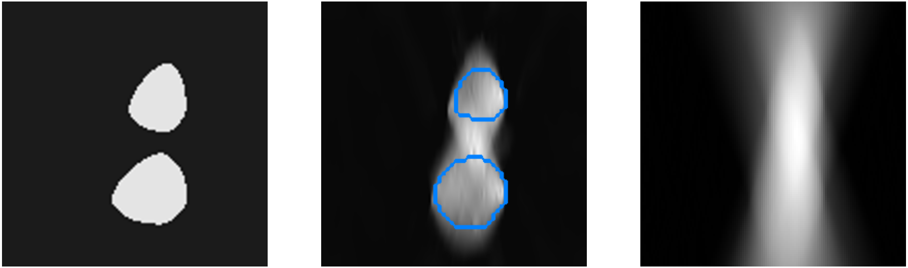

[Rautio, Murthy, Bubba, Lassas and S, submitted]

Outline

Where do we encounter limited-angle tomography?

Industrial case study: low-dose 3D dental X-ray imaging

Matrix-based limited angle tomography and SVD

Ill-posedness of limited-angle Radon transform

Recent progress in limited-angle tomography

- Learning the unknown WF set with shearlets
- Learning the unknown WF set with complex wavelets
- Estimating the unknown WF set with computational topology

Helsinki tomography challenge 2022

Computational homology identifies missing edges

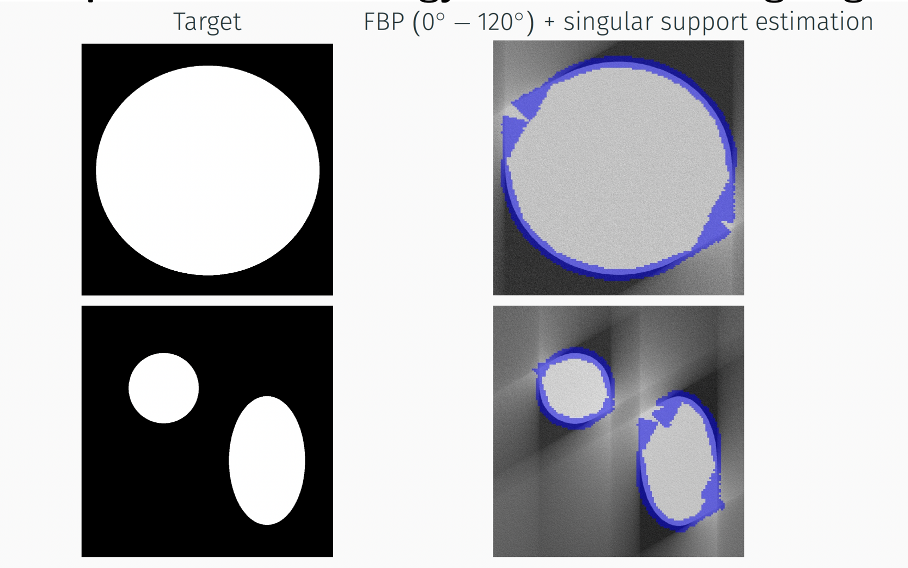

Unpublished work by Elli Karvonen

Outline

Where do we encounter limited-angle tomography?

Industrial case study: low-dose 3D dental X-ray imaging

Matrix-based limited angle tomography and SVD

Ill-posedness of limited-angle Radon transform

Recent progress in limited-angle tomography
- Learning the unknown WF set with shearlets
- Learning the unknown WF set with complex wavelets
- Estimating the unknown WF set with computational topology

Helsinki tomography challenge 2022

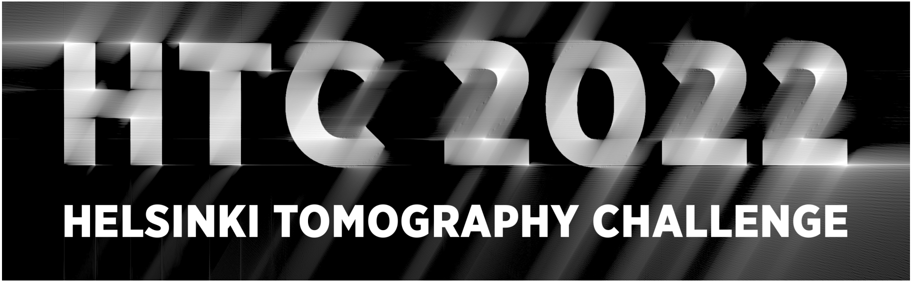

Check it out: https://www.fips.fi/HTC2022.php

Challenge production team: Alexander Meaney, Fernando Moura, Siiri Rautio, Salla Latva-Äijö, Tommi Heikkilä and S.

Limited angle tomography is difficult

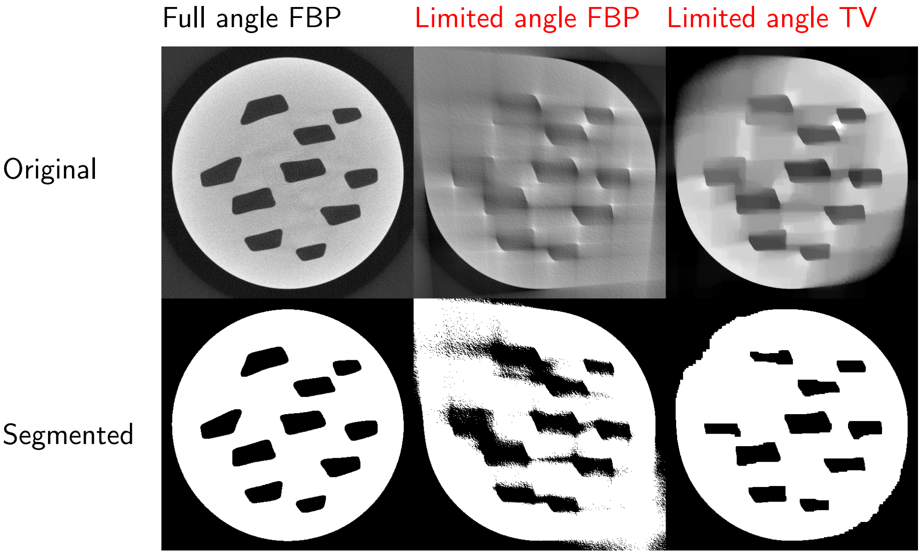

See [Greenleaf & Uhlmann 1989], [Quinto 1993], and [Frikel & Quinto 2013]

We made several plastic phantoms with differently shaped holes in them

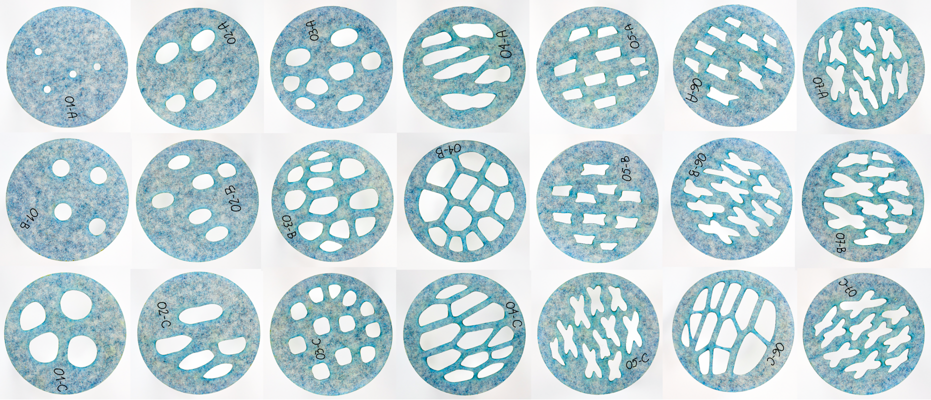

Shown are segmented FBP reconstructions from full-angle data

We measured full-angle X-ray data of the discs using our lab in Helsinki

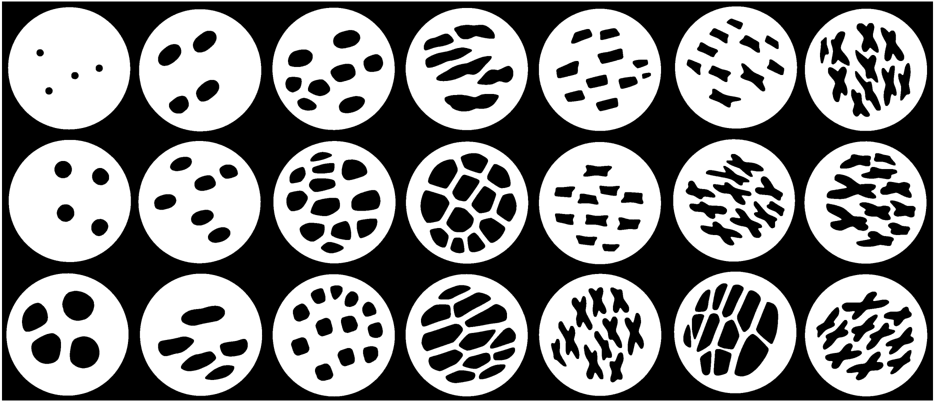

Shown are segmented FBP reconstructions from full-angle data

The difficulty of reconstruction was raised by limiting the angle of view step by step

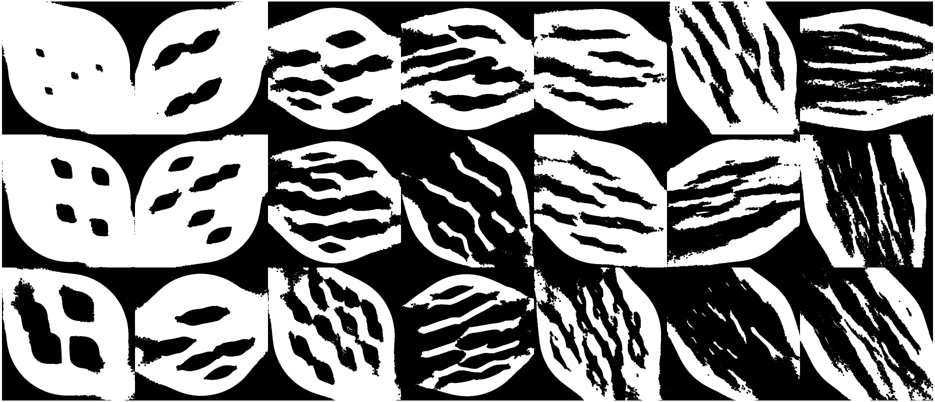

Shown are segmented FBP reconstructions from limited-angle data.
Angular ranges were $90^\circ \to 80^\circ \to \ldots \to 30^\circ$

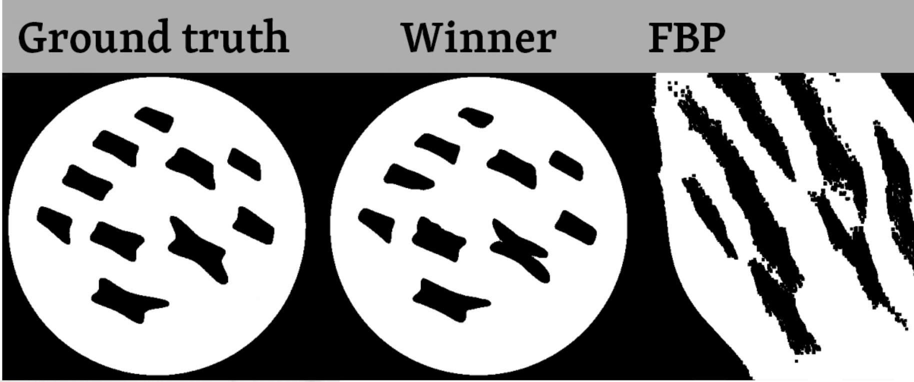
Ground truth
Winner
FBP

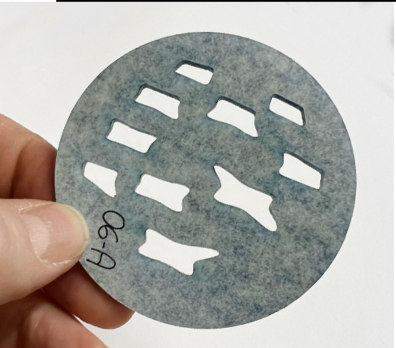
06-A

Helsinki Tomography Challenge 2022: phantom difficulty groups

Group	Angular range	Angle increment	Number of projections
1	90°	0.5	181
2	80°	0.5	161
3	70°	0.5	141
4	60°	0.5	121
5	50°	0.5	101
6	40°	0.5	81
7	30°	0.5	61

The Helsinki Tomography Challenge 2022

9 particapting teams from **7** countries:

- Austria
- Brazil
- China
- Denmark
- Germany
- India
- Singapore

Altogether **22** different algorithms were submitted.

The Helsinki Tomography Challenge 2022

The top ranking teams are:

1. Technical University Dortmund, Department of Computer Science & Heinrich Heine University Düsseldorf, Department of Computer Science - Germany
2. University of Bremen, Center for Industrial Mathematics (ZeTeM) - Germany
3. Technical University of Denmark, Department of Applied Mathematics and Computer Science - Denmark

The full results are viewable at https://fips.fi/HTC2022_results.pdf.

All the data and participating algorithms are openly available.

Scoring the quality of reconstructions

Reconstructed binary image is I_r, ground truth binary image is I_t. The score of the reconstruction is given by the Matthews correlation coefficient (MCC). Define

$$TP = \sum_{i,j} (I_t \cap I_r)_{ij}, \qquad FP = \sum_{i,j} (\bar{I}_t \cap I_r)_{ij},$$

$$FN = \sum_{i,j} (I_t \cap \bar{I}_r)_{ij}, \qquad TN = \sum_{i,j} (\bar{I}_t \cap \bar{I}_r)_{ij}.$$

Calculate MCC score $S \in [-1, 1]$ as

$$S = \frac{TP \times TN - FP \times FN}{\sqrt{(TP + FP)(TP + FN)(TN + FP)(TN + FN)}}.$$

A score of $+1$ (best) represents a perfect reconstruction, 0 no better than random reconstruction, and -1 (worst) indicates total disagreement between reconstruction and ground truth.

The scores of the five best teams in HTC2022

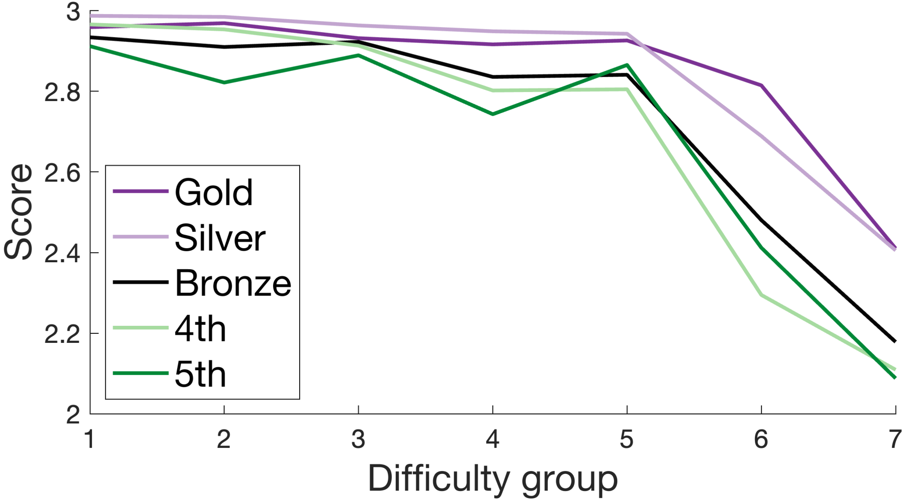

Thank you for your attention!

⟵ Slime mold called Lycogala conicum

Thank you for your attention!